

Supporting Information

Designed Metal-organic π -clusters Combining Aromaticity of Metal Cluster and Ligands for Third-order Nonlinear Optical Response

Zirui Wang^{a,b}, Yayu Yan^{a,c}, Jiali Chen^{a,c}, Qiao-Hong Li^{*,a,d} and Jian Zhang^{*,a,b,d}

^a State Key Laboratory of Structural Chemistry, Fujian Institute of Research on the Structure of Matter, Chinese Academy of Sciences, Fuzhou, Fujian 350002, China

^b School of Physical Science and Technology, ShanghaiTech University, Shanghai 201210, China

^c College of Chemistry, Fuzhou University, Fuzhou, Fujian 350108, China

^d Fujian College, University of Chinese Academy of Sciences, Fuzhou, Fujian 350002, China

E-mail: lqh2382@fjirsm.ac.cn, zhj@fjirsm.ac.cn

Table of Content

Computational details	S3
Table S1. Os-Os Bond Lengths of Different Os-organic π -clusters.	S5
Table S2. Os-Os Bond Angle of Different Os-organic π -clusters.....	S6
Table S3. NPA Charge of Different Os-organic π -clusters.	S7
Table S4. Calculated Formation Free Energy of Different Os-organic π -clusters.	S8
Table S5. Nucleus-Independent Chemical Shift of Different Os-organic π -clusters....	S9
Figure S1. Analysis of the aromaticity of Os-organic π -clusters: Structures (line 2). The π contribution of anisotropy of the induced current density (AICD- π , iso=0.03 a.u.) (line 3). Iso-chemical shielding surfaces in Z direction (ICSS _{ZZ}) (line 4).	S9
Table S6. Third-order NLO Coefficients of Different Os-organic π -clusters.	S10
Figure S2. Third-order NLO coefficients of different Os-organic π -clusters.	S10
Table S7. Molecular Orbitals Energy and HOMOs Components of Different Os- organic π -clusters.	S11
Figure S3. Density of states (DOS) of different Os-organic π -clusters.....	S12
Figure S4. Atomic orbitals of C and Os.....	S12
Figure S5. Normalized UV-vis absorption spectra and electron-hole distribution smoothing isosurface schematic of Os-organic clusters (in).	S13
Figure S6. Normalized UV-vis absorption spectra in the visible-light range of Os ₅ cluster.....	S13
Figure S7. Schematic for dipolar (left), quadrupole (middle), and octupole (right) molecular unit.	S14
Table S8. The Transition Nature of the Major Electron Excitations.	S15
Table S9. Electron-hole Analysis of Main Excited States of Different Os-organic π - clusters.	S16
Table S10. Contribution Ratio of Cluster Cores and Ligands to Electron-hole Distribution.....	S17

Computational details

All the calculations were implemented in Gaussian 16¹. The ground-state equilibrium geometries of these structures were fully optimized with density functional theory (DFT) using B3LYP functional and 6-31G(d,p) basis sets for C, H, and Lanl2DZ basis set for Os with D3 dispersion correction of Grimme²⁻¹⁰. The analysis of nucleus-independent chemical shift (NICS)^{11, 12} were also using B3LYP functional and 6-311++G(d,p) basis sets for C, H. Anisotropy of the Induced Current Density (AICD)^{13, 14} and iso chemical shielding surface (ICSS)^{15, 16} analysis used 6-31+G(d,p) basis sets for C, H. The static third-order nonlinear polarizability calculations and TDDFT were used cam-B3LYP functional¹⁷ and aug-cc-pVDZ basis set for C, H. The frequency-dependent second hyperpolarizabilities were calculated by the sum-over-states (SOS) method^{18, 19}. In order to get a deeper understanding of the wave function, Multiwfn 3.8(dev) code²⁰ and VMD software²¹ were used to analyze the electronic structures, hyperpolarizability, excitation characteristics, and aromaticity.

The electron–hole distributions are defined as follows:

$$\rho^{hole}(r) = \sum_{i \rightarrow a} (w_i^a)^2 \phi_i(r) \phi_i(r) + \sum_{i \rightarrow a} \sum_{j \neq i \rightarrow a} w_i^a w_j^a \phi_i(r) \phi_j(r)$$

$$\rho^{electron}(r) = \sum_{i \rightarrow a} (w_i^a)^2 \phi_a(r) \phi_a(r) + \sum_{i \rightarrow a} \sum_{i \rightarrow b \neq a} w_i^a w_i^b \phi_a(r) \phi_b(r)$$

where i and j are the occupied orbital labels, a and b are the virtual orbital labels, and ϕ is the orbital wave function. w corresponds to the configuration coefficient of excitation.

The D index is used to measure the distance between the center of mass of holes and electrons.

$$D = \sqrt{(X_{ele} - X_{hole})^2 + (Y_{ele} - Y_{hole})^2 + (Z_{ele} - Z_{hole})^2}$$

The t index is used to measure the separation degree of holes and electrons.

$$t = D - H_{CT}$$

E_{coul} represents the electron–hole coulomb attractive energy.

$$E_{coul} = \iint \frac{\rho^{hole}(r_1)\rho^{ele}(r_2)}{|r_1 - r_2|} dr_1 dr_2$$

The hole delocalization index (*HDI*) and the electron delocalization index (*EDI*) are

$$HDI = 100 \times \sqrt{\int [\rho^{hole}(r)]^2 dr}$$

$$EDI = 100 \times \sqrt{\int [\rho^{ele}(r)]^2 dr}$$

Table S1. Os-Os Bond Lengths of Different Os-organic π -clusters.

Cluster	Os-Os bond length/ \AA								Average/ \AA	
Os₃	Os1-Os2	Os2-Os3	Os3-Os1							
	2.479	2.386	2.716							
Os₄	Os1-Os2	Os2-Os3	Os3-Os4	Os4-Os1						
	2.462	2.462	2.462	2.461						
Os₅	Os1-Os2	Os2-Os3	Os3-Os4	Os4-Os5	Os5-Os1					
	2.567	2.408	2.481	2.457	2.440					
Os₆	Os1-Os2	Os2-Os3	Os3-Os4	Os4-Os5	Os5-Os6	Os6-Os1				
	2.428	2.429	2.428	2.428	2.428	2.428				
Os₇	Os1-Os2	Os2-Os3	Os3-Os4	Os4-Os5	Os5-Os6	Os6-Os7	Os7-Os1			
	2.433	2.429	2.439	2.437	2.426	2.418	2.425			
Os₈	Os1-Os2	Os2-Os3	Os3-Os4	Os4-Os5	Os5-Os6	Os6-Os7	Os7-Os8	Os8-Os1		
	2.420	2.419	2.420	2.419	2.420	2.420	2.418	2.420		
Os₉	Os1-Os2	Os2-Os3	Os3-Os4	Os4-Os5	Os5-Os6	Os6-Os7	Os7-Os8	Os8-Os9	Os9-Os1	2.415
	2.420	2.411	2.413	2.399	2.394	2.445	2.413	2.428	2.416	

Table S2. Os-Os Bond Angle of Different Os-organic π -clusters.

Cluster	Os-Os bond angle/ $^{\circ}$							Average/ \AA		
Os₃	Os1-Os2-Os3	Os1-Os3-Os2	Os2-Os1-Os3	-	-	-	-	60.0		
	67.9	57.7	54.5							
Os₄	Os1-Os2-Os3	Os2-Os3-Os4	Os3-Os4-Os1	Os4-Os1-Os2	-	-	-	88.7		
	88.7	88.7	88.7	88.7						
Os₅	Os1-Os2-Os3	Os2-Os3-Os4	Os3-Os4-Os5	Os4-Os5-Os1	Os5-Os1-Os2	-	-	103.0		
	107.4	98.0	106.5	97.5	105.8					
Os₆	Os1-Os2-Os3	Os2-Os3-Os4	Os3-Os4-Os5	Os4-Os5-Os6	Os5-Os6-Os1	Os6-Os1-Os2	-	109.2		
	109.2	109.2	109.3	109.2	109.2	109.3				
Os₇	Os1-Os2-Os3	Os2-Os3-Os4	Os3-Os4-Os5	Os4-Os5-Os6	Os5-Os6-Os7	Os6-Os7-Os1	Os7-Os1-Os2	-		
	114.8	121.6	112.3	116.7	112.4	112.9	115.4	115.1		
Os₈	Os1-Os2-Os3	Os2-Os3-Os4	Os3-Os4-Os5	Os4-Os5-Os6	Os5-Os6-Os7	Os6-Os7-Os8	Os7-Os8-Os1	Os8-Os1-Os2	-	
	117.7	117.4	117	117.4	117.6	117.3	117.1	117.3	117.3	
Os₉	Os1-Os2-Os3	Os2-Os3-Os4	Os3-Os4-Os5	Os4-Os5-Os6	Os5-Os6-Os7	Os6-Os7-Os8	Os7-Os8-Os9	Os8-Os9-Os1	Os9-Os1-Os2	-
	117.6	123.3	117.1	124.1	126.1	117.4	119.7	120.9	120.9	120.8

Table S3. NPA Charge of Different Os-organic π -clusters.

Cluster	Os1	Os2	Os3	Os4	Os5	Os6	Os7	Os8	Os9	sum
Os₃	0.241	-0.022	0.081	-	-	-	-	-	-	0.300
Os₄	0.024	0.024	0.024	0.025	-	-	-	-	-	0.097
Os₅	0.129	0.020	0.059	-0.014	0.126	-	-	-	-	0.320
Os₆	0.063	0.063	0.063	0.063	0.064	0.063	-	-	-	0.379
Os₇	0.077	0.019	0.059	0.068	0.051	-0.002	0.084	-	-	0.356
Os₈	0.046	0.051	0.053	0.050	0.048	0.049	0.054	0.051	-	0.402
Os₉	0.089	0.058	0.029	0.020	0.065	0.020	0.065	0.040	-0.009	0.377

Table S4. Calculated Formation Free Energy of Different Os-organic π -clusters.

Cluster	N \times Os ₁ /Hartree	Zero-point correction /Hartree	Electronic and zero- point Energies /Hartree	Electronic /Hartree	Electronic and thermal Free Energies /Hartree	Thermal Free Energies /Hartree	G /Hartree	ΔG /Hartree	$\Delta G_{\text{average}}$ /Hartree
Os ₁	-361.099	0.101	-361.167	-361.269	-361.200	0.069	-361.099	0.000	0.000
Os ₃	-1083.297	0.311	-1083.780	-1084.091	-1083.835	0.256	-1083.524	-0.227	-0.076
Os ₄	-1444.396	0.416	-1445.111	-1445.526	-1445.175	0.351	-1444.759	-0.363	-0.091
Os ₅	-1805.495	0.520	-1806.395	-1806.914	-1806.469	0.445	-1805.949	-0.455	-0.091
Os ₆	-2166.594	0.627	-2167.731	-2168.359	-2167.810	0.548	-2167.183	-0.589	-0.098
Os ₇	-2527.693	0.734	-2529.016	-2529.750	-2529.106	0.644	-2528.372	-0.679	-0.097
Os ₈	-2888.792	0.840	-2890.334	-2891.174	-2890.433	0.741	-2889.593	-0.801	-0.100
Os ₉	-3249.891	0.947	-3251.623	-3252.570	-3251.731	0.839	-3250.784	-0.893	-0.099

Table S5. Nucleus-Independent Chemical Shift of Different Os-organic π -clusters.

Cluster	NICS(0) /ppm	NICS(1) /ppm	NICS(0) _{zz} /ppm	NICS(1) _{zz} /ppm	NICS(0) _{nzz} /ppm	NICS(1) _{nzz} /ppm
Os₃	-18.51	-17.22	-96.62	-35.29	-54.45	-27.05
Os₄	-21.11	-19.33	-87.78	-49.69	-59.40	-38.18
Os₅	-9.37	-4.20	-42.28	-20.78	-27.59	-13.04
Os₆	2.25	4.00	-6.11	-0.96	-10.01	-6.15
Os₇	2.54	4.48	-8.17	-6.34	-22.42	-17.39
Os₈	0.41	2.36	-8.02	-5.91	-22.30	-17.40
Os₉	5.30	4.92	-2.65	-3.92	-11.48	-10.28

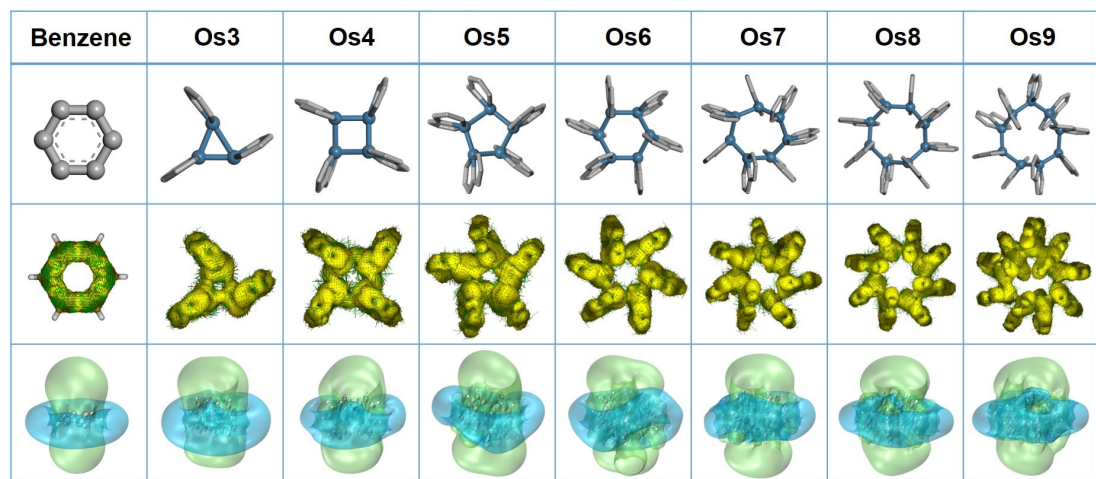


Figure S1. Analysis of the aromaticity of Os-organic π -clusters: Structures (line 2). The π contribution of anisotropy of the induced current density (AICD- π , iso=0.03 a.u.) (line 3). Iso-chemical shielding surfaces in the Z direction (ICSS_{zz}) (line 4).

Table S6. Third-order NLO Coefficients of Different Os-organic π -clusters.

Cluster	Magnitude of gamma/a.u.	Average of Magnitude of gamma/a.u.
Os₃	7.610900E+04	2.536967E+04
Os₄	1.001181E+05	2.502953E+04
Os₅	1.640102E+05	3.280204E+04
Os₆	1.398585E+05	2.330975E+04
Os₇	1.708772E+05	2.441103E+04
Os₈	1.997905E+05	2.497381E+04
Os₉	2.443956E+05	2.715507E+04

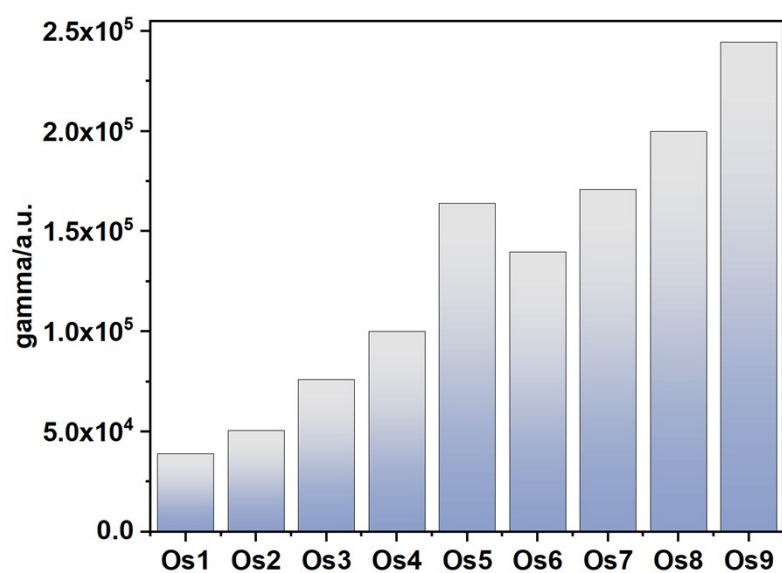


Figure S2. Third-order NLO coefficients of different Os-organic π -clusters.

Table S7. Molecular Orbitals Energy and HOMOs Components of Different Os-organic π -clusters.

Cluster	HOMO/eV	LUMO/eV	E_{gap}/eV	Os (5d)	C (2p)	Other
Os₁	-4.71	-2.03	2.68	68.64%	2.26%	29.10%
Os₃	-4.98	-2.86	2.13	74.39%	13.73%	11.88%
Os₄	-4.92	-2.58	2.34	53.86%	38.45%	7.69%
Os₅	-4.32	-2.86	1.47	41.86%	44.13%	14.01%
Os₆	-4.60	-2.40	2.20	39.80%	41.46%	18.74%
Os₇	-4.42	-2.53	1.88	48.04%	34.21%	17.75%
Os₈	-4.70	-2.27	2.43	45.84%	32.47%	21.69%
Os₉	-4.29	-2.60	1.69	44.05%	32.62%	23.33%

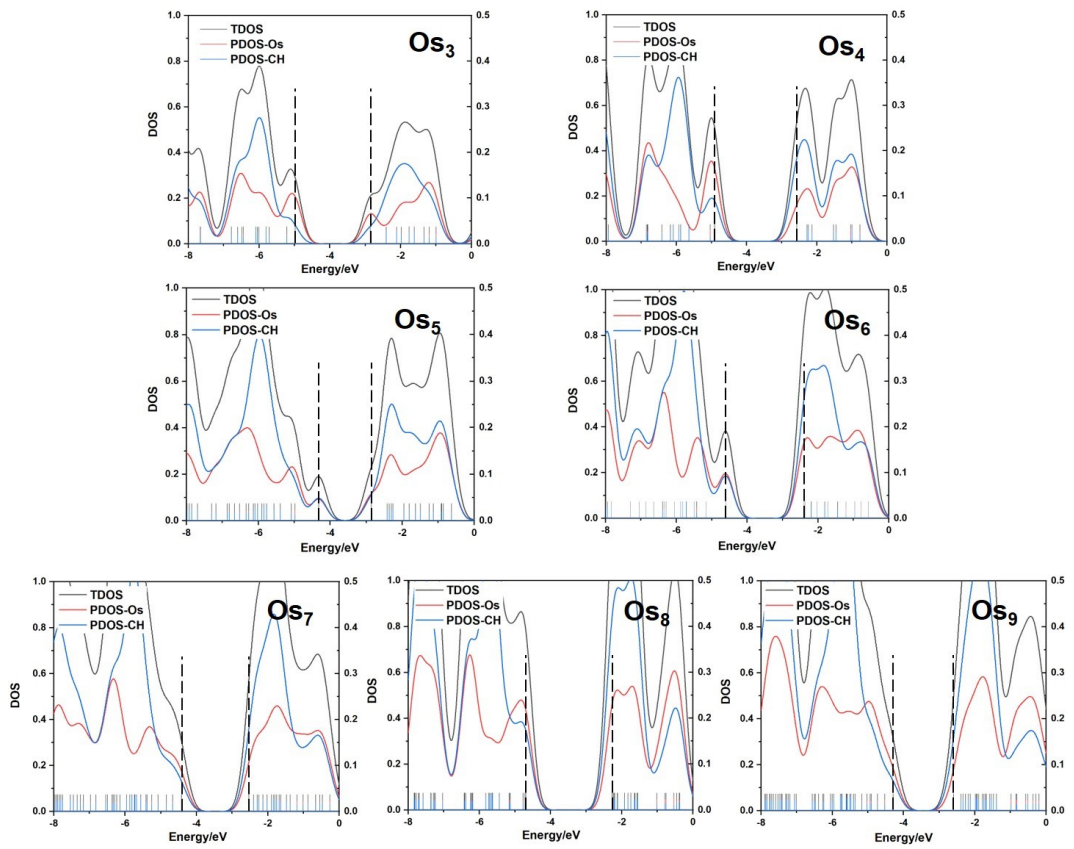


Figure S3. Density of states (DOS) of different Os-organic π -clusters.

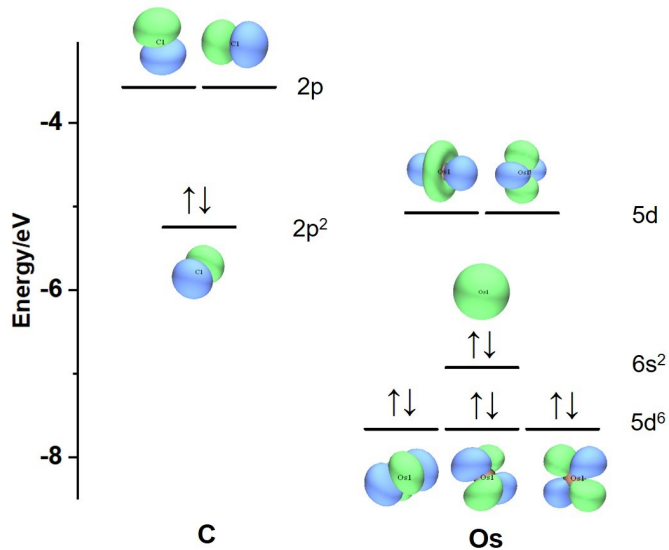


Figure S4. Atomic orbitals of C and Os.

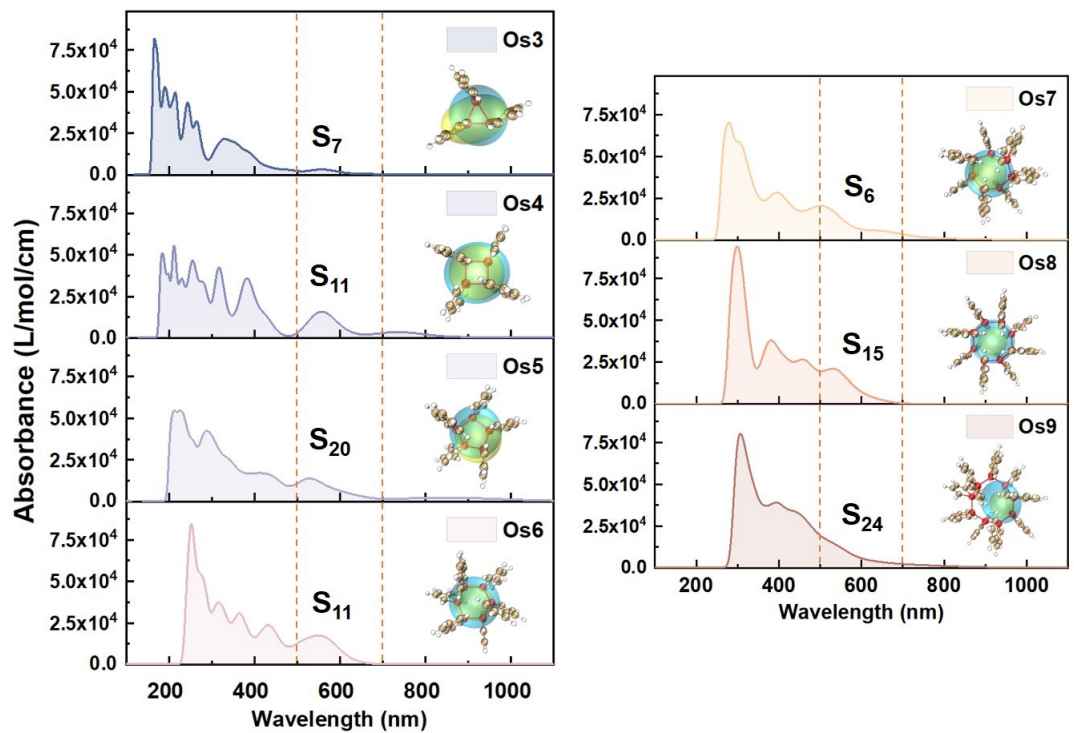


Figure S5. Normalized UV-vis absorption spectra and electron-hole distribution smoothing isosurface schematic of Os-organic clusters (in).

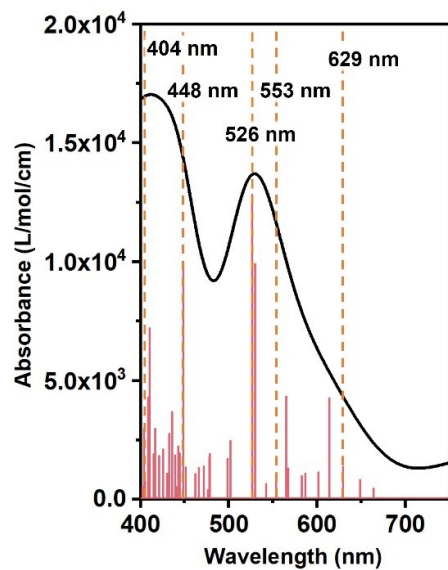


Figure S6. Normalized UV-vis absorption spectra in the visible-light range of the Os_5 cluster.

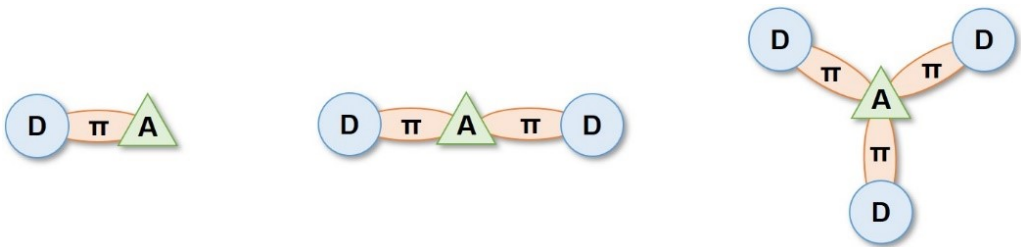


Figure S7. Schematic for dipolar (left), quadrupole (middle), and octupole (right) molecular unit.

Table S8. The Transition Nature of the Major Electron Excitations.

Cluster	Wavelength	f	Major MO transitions
Os ₃	S ₀ -S ₇ : 558.69 nm	0.02600	H-1 -> L+1 72.0%, H-1 -> L+6 7.6%, H-1 -> L+2 5.8%
Os ₄	S ₀ -S ₁₁ : 564.05 nm	0.06670	H-2 -> L+2 45.6%, H-2 -> L+3 31.7%
Os ₅	S ₀ -S ₂₀ : 526.05 nm	0.06410	H -> L+8 24.2%, H -> L+6 14.9%, H-2 -> L+1 7.6%, H-3 -> L+1 6.9%
Os ₆	S ₀ -S ₁₁ : 566.53 nm	0.07730	H-1 -> L+3 25.1%, H -> L+4 25.0%, H -> L+5 14.9%, H-4 -> L 9.0%, H-2 -> L+1 8.2%
Os ₇	S ₀ -S ₆ : 654.03 nm	0.02240	H-1 -> L+2 19.9%, H-2 -> L 12.7%, H-1 -> L+1 10.5%, H -> L+3 5.4%, H-3 -> L 5.3%, H-2 -> L+1 5.1%
Os ₈	S ₀ -S ₁₅ : 545.92 nm	0.07900	H -> L+7 10.6%, H-3 -> L+5 7.4%, H-2 -> L+6 6.4%, H-2 -> L+5 6.3%, H-3 -> L+6 5.7%
Os ₉	S ₀ -S ₂₄ : 544.94 nm	0.01000	H-1 -> L+15 14.7%, H -> L+10 7.6%, H -> L+15 5.6%

Table S9. Electron-hole Analysis of Main Excited States of Different Os-organic π -clusters.

Cluster	Wavelength	S_r (a.u.)	D (\AA)	H (\AA)	t (\AA)	HDI	EDI	E_{coul} (eV)
Os_3	S_0-S_7 : 558.69 nm	0.75	0.548	2.87	-1.24	6.56	6.03	4.88
Os_4	S_0-S_{11} : 564.05 nm	0.83	0.223	3.19	-1.10	6.37	4.01	4.46
Os_5	S_0-S_{20} : 526.05 nm	0.85	0.868	3.44	-1.29	4.23	3.85	4.08
Os_6	S_0-S_{11} : 566.53 nm	0.85	0.001	3.74	-2.46	3.63	3.15	3.81
Os_7	S_0-S_6 : 654.03 nm	0.82	0.209	3.86	-2.05	3.74	3.71	3.70
Os_8	S_0-S_{15} : 545.92 nm	0.87	0.051	4.14	-1.90	3.17	2.82	3.47
Os_9	S_0-S_{24} : 544.94 nm	0.80	0.492	4.20	-2.23	4.37	3.66	3.42

Table S10. Contribution Ratio of Cluster Cores and Ligands to Electron-hole Distribution.

Cluster	Wavelength	% <i>Ele_M</i>	% <i>Ele_L</i>	% <i>Hole_M</i>	% <i>Hole_L</i>	<i>Ele_M-0.5</i>	<i>Ele_L-0.5</i>	<i>Hole_M-0.5</i>	<i>Hole_L-0.5</i>	Σ
Os ₃	S ₀ -S ₇ : 558.69 nm	32.08%	67.92%	55.34%	44.66%	0.1792	0.1792	0.0534	0.0534	0.4652
Os ₄	S ₀ -S ₁₁ : 564.05 nm	37.73%	62.27%	71.79%	28.20%	0.1227	0.1227	0.2179	0.2180	0.6813
Os ₅	S ₀ -S ₂₀ : 526.05 nm	36.93%	63.07%	57.39%	42.61%	0.1307	0.1307	0.0739	0.0739	0.4092
Os ₆	S ₀ -S ₁₁ : 566.53 nm	34.85%	65.15%	68.34%	31.66%	0.1515	0.1515	0.1834	0.1834	0.6698
Os ₇	S ₀ -S ₆ : 654.03 nm	41.50%	58.50%	75.16%	24.84%	0.0850	0.0850	0.2516	0.2516	0.6732
Os ₈	S ₀ -S ₁₅ : 545.92 nm	49.05%	50.95%	71.27%	28.73%	0.0095	0.0095	0.2127	0.2127	0.4444
Os ₉	S ₀ -S ₂₄ : 544.94 nm	45.01%	54.99%	85.36%	14.64%	0.0499	0.0499	0.3536	0.3536	0.8070

References

1. M. J. Frisch, G. W. Trucks, H. B. Schlegel, G. E. Scuseria, M. A. Robb, J. R. Cheeseman, G. Scalmani, V. Barone, G. A. Petersson, H. Nakatsuji, X. Li, M. Caricato, A. V. Marenich, J. Bloino, B. G. Janesko, R. Gomperts, H. P. H. B. Mennucci, A. F. I. J. V. Ortiz, J. L. Sonnenberg, and F. D. D. Williams-Young, F. Lipparini, F. Egidi, J. Goings, B. Peng, A. Petrone, T. Henderson, D. Ranasinghe, V. G. Zakrzewski, J. Gao, N. Rega, G. Zheng, W. Liang, M. Hada, M. Ehara, K. Toyota, R. Fukuda, J. Hasegawa, M. Ishida, T. Nakajima, Y. Honda, O. Kitao, H. Nakai, T. Vreven, K. Throssell, J. A. Montgomery, Jr., J. E. Peralta, F. Ogliaro, M. J. Bearpark, J. J. Heyd, E. N. Brothers, K. N. Kudin, V. N. Staroverov, T. A. Keith, R. Kobayashi, J. Normand, K. Raghavachari, A. P. Rendell, J. C. Burant, S. S. Iyengar, J. Tomasi, M. Cossi, J. M. Millam, M. Klene, C. Adamo, R. Cammi, J. W. Ochterski, R. L. Martin, K. Morokuma, O. Farkas, J. B. Foresman, and D. J. Fox, *Journal*, 2016.
2. P. J. Hay and W. R. Wadt, *J. Chem. Phys.*, 1985, **82**, 270-283.
3. W. R. Wadt and P. J. Hay, *J. Chem. Phys.*, 1985, **82**, 284-298.
4. P. J. Hay and W. R. Wadt, *J. Chem. Phys.*, 1985, **82**, 299-310.
5. A. D. Becke, *Phys. Rev. A* , 1988, **38**, 3098-3100.
6. C. T. Lee, W. T. Yang and R. G. Parr, *Phys. Rev. B* , 1988, **37**, 785-789.
7. B. Miehlich, A. Savin, H. Stoll and H. Preuss, *Chem. Phys. Lett.*, 1989, **157**, 200-206.
8. A. D. Becke, *J. Chem. Phys.*, 1993, **98**, 1372-1377.
9. P. J. Stephens, F. J. Devlin, C. F. Chabalowski and M. J. Frisch, *J. Phys. Chem.*, 1994, **98**, 11623-11627.
10. S. Grimme, J. Antony, S. Ehrlich and H. Krieg, *J. Chem. Phys.*, 2010, **132**.
11. P. v. R. Schleyer, C. Maerker, A. Dransfeld, H. Jiao and N. J. R. van Eikema Hommes, *J. Am. Chem. Soc.*, 1996, **118**, 6317-6318.
12. Z. Chen, C. S. Wannere, C. Corminboeuf, R. Puchta and P. v. R. Schleyer, *Chem. Rev.*, 2005, **105**, 3842-3888.
13. R. Herges and D. Geuenich, *J. Phys. Chem. A*, 2001, **105**, 3214-3220.
14. D. Geuenich, K. Hess, F. Köhler and R. Herges, *Chem. Rev.*, 2005, **105**, 3758-3772.
15. S. Klod and E. Kleinpeter, *J. Chem. Soc., Perkin Trans. 2*, 2001, DOI: 10.1039/B009809O, 1893-1898.
16. Z. Liu, T. Lu and Q. Chen, *Carbon*, 2020, **165**, 468-475.
17. T. Yanai, D. P. Tew and N. C. Handy, *Chem. Phys. Lett.*, 2004, **393**, 51-57.
18. K. Sasagane, F. Aiga and R. Itoh, *J. Chem. Phys.*, 1993, **99**, 3738-3778.
19. F. Meyers, S. R. Marder, B. M. Pierce and J. L. Bredas, *J. Am. Chem. Soc.*, 1994, **116**, 10703-10714.
20. T. Lu and F. Chen, *J. Comput. Chem.*, 2012, **33**, 580-592.
21. W. Humphrey, A. Dalke and K. Schulten, *J. Mol. Graph.*, 1996, **14**, 33-38.